

Porous yttria-stabilized zirconia ceramics with ultra-low thermal conductivity

LiangFa Hu · Chang-An Wang · Yong Huang

Received: 7 November 2009 / Accepted: 16 February 2010 / Published online: 5 March 2010
© Springer Science+Business Media, LLC 2010

Abstract Porous yttria-stabilized zirconia (ZrO_2 -8 mol% Y_2O_3 , YSZ) ceramics with ultra-low thermal conductivity (as low as 0.06 W/mK) could be fabricated by tert-butyl alcohol (TBA)-based gel-casting process with low solid loadings of 10 and 15 vol%. High porosity (52–76%) and fine pores with average pore size of 0.7–1.8 μm formed after sintering at 1350–1550 °C. These air-containing pores were believed to affect the through-thickness heat transfer propagation, resulting in low thermal conductivity. The thermal conductivity of porous YSZ ceramics with different porosities fits well with computed values derived from Effective Medium Theory (EMT).

Introduction

Due to industrial applications of porous zirconia ceramics in ceramic filters, catalyst supports, solid oxide fuel cells, biological materials, and thermal barrier [1, 2], several fabrication methods have been employed, including: colloidal process; using polymethylmethacrylate powder as a pore-forming agent; direct casting; graphite template-based dip-coating; freeze casting; tape-casting; infiltration of zirconium oxychloride ($\text{ZrOCl}_2 \cdot 8\text{H}_2\text{O}$) sol into biological template structures; pore formation with hydrogen peroxide; and water-based gel-casting [2–10]. Additional research has focused on zirconia thermal barrier coatings

for applications in thermal insulation. However, few studies report on the applications of porous zirconia ceramics in bulk thermal isolators [11, 12].

Fully stabilized zirconia is one of the best crystalline thermal insulators known. Partially stabilized zirconia, which offers low thermal conductivity and good mechanical performance, is of great interest for thermal isolation in high-temperature processes, insulated engine components, refractory and thermal insulation [13]. Furthermore, introducing pores to the zirconia materials further decreases thermal conductivity, because air trapped in the pores is a better thermal insulator. Therefore, fabrication of porous zirconia ceramics with a low thermal conductivity is important for its applications in bulk thermal isolators.

Recently, porous zirconia ceramics with low thermal conductivities (0.13–0.55 W/mK, the lowest level so far) were prepared by using latex as the pore former [14], but the nanoparticles used significantly increase the cost. In this paper, porous YSZ ceramics were successfully fabricated from micro-sized powders based on the TBA-based gel-casting method which is a recently developed method for fabricating highly porous ceramics [15]. A lower limit of thermal conductivity (0.06 W/mK) was approached. The ceramic microstructure, thermal conductivity at room temperature, and compressive strength were investigated.

Many proposed studies have sought to understand the effects of porosity on the thermal conductivity of a two-component material system, including the Maxwell-Eucken model [16] and the Effective Medium Theory (EMT) [17]. In this paper, these models were applied to porous YSZ ceramics, and the experimental data and theoretical values derived from the EMT equation were compared and discussed.

L. Hu · C.-A. Wang (✉) · Y. Huang
Department of Materials Science and Engineering, State Key
Lab of New Ceramics and Fine Processing, Tsinghua University,
Beijing 100084, People's Republic of China
e-mail: wangca@tsinghua.edu.cn; huliangfa@gmail.com

Experimental procedure

Materials

Commercially available yttria-stabilized zirconia (ZrO_2 -8 mol% Y_2O_3 , YSZ) powder (AR grade, Shanghai Chemical Regent Co., China) was used as the starting material. This YSZ powder has an average particle size of 1.26 μm and a specific surface area of 6.49 m^2/g . Tert-butyl alcohol (TBA, chemical purity, Beijing Yili Chemical Co., Beijing, China) was used as shaping solvent and pore forming agent in gel-casting process. A premix solution of monomers and cross linker was prepared in TBA with a concentration of 14.5 wt% of acrylamide (AM, $C_2H_3CONH_2$) and 0.5 wt% N,N'-methylenebisacrylamide (MBAM, $(C_2H_3CONH)_2CH_2$). Initiator and catalyst for gelation reaction are ammonium persulfate (APS) and N,N,N,N-tetramethylethylenediamine (TEMED), respectively. All chemicals used in this study are analytical grade.

Fabrication procedure

The TBA-based gel-casting technique typically consists of preparing a liquid suspension (slurry), molding, drying, binder removal, and sintering. Slurries with 10 and 15 vol% solid loading, including YSZ powders, TBA, acrylamide (AM) were prepared by ball milling for 5 h. To adjust the suspension to a proper flowability during casting, selected alkali solution was added into the slurries. After ball milling, initiator and catalyst were mixed into the slurries. These slurries were poured into molds and dried at 52 °C in nitrogen atmosphere. During the drying procedure, the polymerization of AM occurred and TBA gradually volatilized. Green bodies were then produced. Subsequently, they were sintered at different temperatures of 1350, 1400, 1450, 1500, and 1550 °C for 2 h.

Characterization

Pore size distribution was analyzed by the mercury intrusion method (AutoPore IV 9510). The porosity was calculated using mass and volume measurements to determine the density of the porous samples and then comparing this to the density of the fully dense ceramic, which was taken as 6.0 g/cm^3 for this YSZ material. Three specimens were used to determine the average porosity. Microstructure was observed using a scanning electron microscope (SEM, JSM 6700F, JEOL, Tokyo, Japan). Grain size was determined from the SEM images taken at four locations on each sample (20 grains per location). Thermal conductivity at room temperature was measured on $5 \times 5 \times 3 \text{ mm}^3$ machined specimens, using the Thermal Transport Option

(TTO) of Physical Properties Measurement System (PPMS, Model 6000, Quantum Design, United States). The TTO system measures thermal conductivity λ by applying heat from the heater shoe in order to create a user-specified temperature differential between the two thermometer shoes. The TTO system dynamically models the thermal response of the sample to the low-frequency, square-wave heat pulse, thus expediting data acquisition. TTO can then calculate thermal conductivity directly from the applied heat power, resulting ΔT , and sample geometry. For the compressive strength measurements, samples with a diameter of 20 mm and a height of 20 mm were loaded with a crosshead speed of 0.05 mm/min (CSS-2220 test machine). Three specimens were used to determine the average compressive strength.

Results and discussion

Figure 1 shows the details of pore morphology and interconnection of grains in the sintered ceramics. It was observed that the grains grew up and the porosity decreased as the sintering temperature increased from 1450°C to 1550°C. These change trends could be verified by the determined values of grain size and porosity presented in Table 1. All samples had homogeneous pore distribution and 3–3 connectivity structure with pore size around 1 μm . Figure 1d shows the typical connectivity of grains from which the sintering neck can be easily observed. The strong network provided by the interconnection of grains made it possible for the bodies to obtain high mechanical strength, easy to handle during the fabrication process and more adaptive to the working condition.

Figure 2 shows the pore size distributions of the porous YSZ specimens with solid loading of 10 vol% and different sintering temperatures. Each case presented a single peak with narrow half-peak width, signifying a uniform pore size distribution. Meanwhile, both the average pore size and the area below the curve (indicating the total volume fraction of the pores) decreased with increasing sintering temperature. It is believed that both more tight connection between grains and growth of grains with increasing temperature (see Fig. 1) accounted for the reduction of pore size.

The measured properties, i.e., porosity, grain size, room-temperature thermal conductivity, and compressive strength, are listed in Table 1. Each entry represented an average of three measurements of three different specimens. The porosity showed considerable variation over the 10 samples. Sample A was the most porous (porosity, 75.9%), owing to the lowest sintering temperature and the lower solid loading. The lowest thermal conductivity was also seen for Sample A. Porosity generally declined with

Fig. 1 SEM images of porous YSZ specimens sintered at different temperatures: **a** 1450 °C, **b** 1500 °C, **c** 1550 °C, and **d** typical interconnection of grains

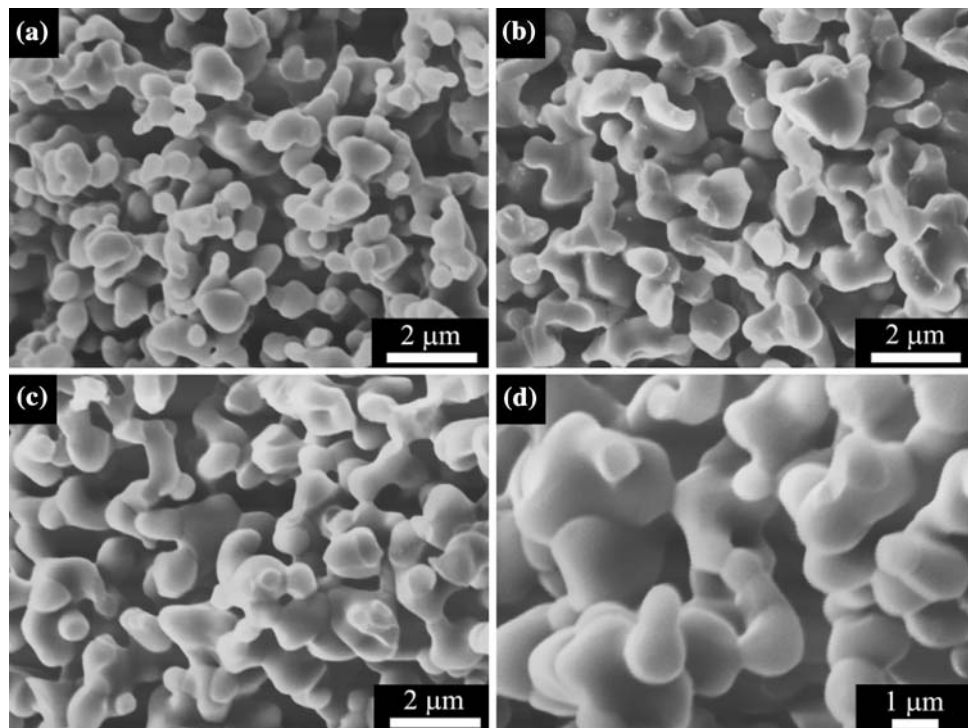


Table 1 Porosity, grain size, room-temperature thermal conductivity, and compressive strength of porous YSZ ceramics with different solid loadings and sintering temperatures

Sample	Solid loading (vol%)	Sintering temperature (°C)	Porosity (%)	Grain size (μm)	Room-temperature thermal conductivity (W/mK)	Compressive strength (MPa)
A	10	1350	75.9 ± 1.6	1.28	0.06 ± 0.04	3.04 ± 0.13
B		1400	74.2 ± 1.4	1.31	0.07 ± 0.02	7.92 ± 0.52
C		1450	72.4 ± 0.2	1.35	0.10 ± 0.06	9.64 ± 1.45
D		1500	66.0 ± 1.1	1.55	0.20 ± 0.09	13.15 ± 0.48
E		1550	65.6 ± 0.4	1.78	0.17 ± 0.06	24.92 ± 2.37
F	15	1350	71.8 ± 1.4	1.30	0.08 ± 0.01	4.12 ± 0.27
G		1400	65.0 ± 2.3	1.33	0.18 ± 0.01	9.22 ± 1.75
H		1450	63.1 ± 2.6	1.46	0.27 ± 0.06	11.19 ± 1.48
I		1500	51.5 ± 4.1	1.57	0.42 ± 0.11	10.66 ± 0.53
J		1550	56.4 ± 3.0	1.62	0.34 ± 0.06	29.01 ± 6.76

increasing temperature, but both grain size and thermal conductivity increased as temperature increased. Samples with 10 vol% solid loading had higher porosities and grain sizes as a whole than samples with 15 vol%, but the former had lower thermal conductivities than the latter. Compressive strength ranged from 3 to 29 MPa, and increased significantly as sintering temperature increased. The authors believe that the increasing sintering temperature led increasingly strong sintering neck and thus increasingly strong network in the sintered bodies, resulting in increasing compressive strength. Meanwhile, the decreased porosity caused by sintering densification left less possibility for cracking

generation and propagation, contributing also to increasing compressive strength.

Figure 3 shows the influence of porosity on the thermal conductivity, together with the predicted values from the Maxwell-Eucken model and the EMT equation. On the basis of the component volume fractions and conductivities, Hashin and Shtrikman [16] derived effective conductivity bounds that were the best (i.e., narrowest) possible bounds for macroscopically homogeneous, isotropic, two-phase materials. Those bounds were mathematically equivalent to the two forms of the well-known Maxwell-Eucken model:

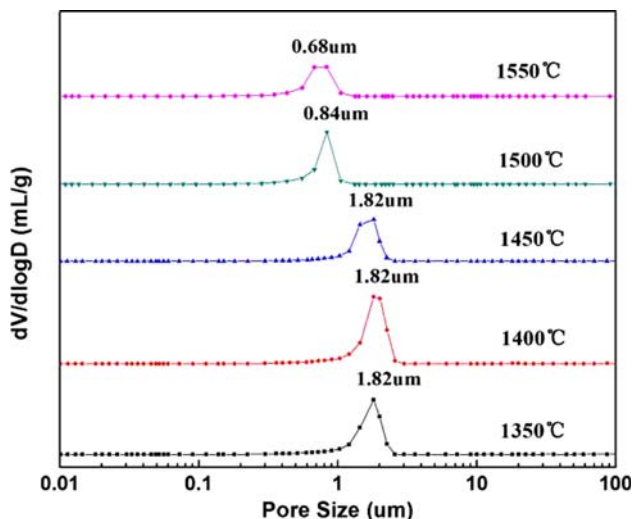


Fig. 2 Pore size distribution of the porous YSZ specimens with solid loading of 10 vol% and different sintering temperatures

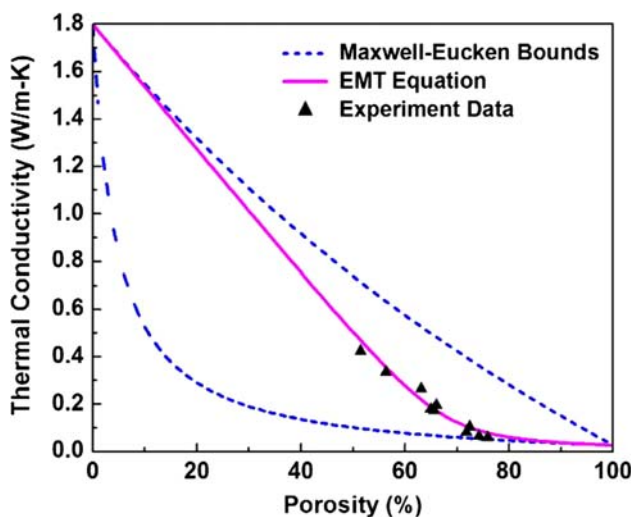


Fig. 3 Comparison of experimental thermal conductivities and theoretical thermal conductivities based on the Maxwell-Eucken model and the EMT equation

Maxwell-Eucken 1:

$$k_e = k_1 \frac{2k_1 + k_2 - 2(k_1 - k_2)v_2}{2k_1 + k_2 + (k_1 - k_2)v_2} \tag{1}$$

Maxwell-Eucken 2:

$$k_e = k_2 \frac{2k_2 + k_1 - 2(k_2 - k_1)(1 - v_2)}{2k_2 + k_1 + (k_2 - k_1)(1 - v_2)} \tag{2}$$

where k and v are thermal conductivity and volume fraction. Subscripts of e , 1, and 2 represent the two-component material, component 1 and component 2, respectively. The thermal conductivity of air and dense YSZ ceramics (with yttria percentage of 8 mol%) were chosen to be 0.026 and 1.8 W/mK from literature values [17, 18].

In a heterogeneous material structure in which the two components are distributed connectively, either component may form continuous heat conduction pathways, depending on the relative amounts of the components. James [19] developed Landauer’s theory [20] and pointed out that the effective conductivity of this type of structure could be modeled well by the EMT equation:

$$(1 - v_2) \frac{k_1 - k_e}{k_1 + 2k_e} + v_2 \frac{k_2 - k_e}{k_2 + 2k_e} = 0 \tag{3}$$

The experimental thermal conductivities fit well with the values computed from the EMT equation, which gave values located between the bounds derived from the Maxwell-Eucken model. The initial thermal conductivity of fully dense YSZ ceramics (with yttria percentage of 8 mol%) was about 1.8 W/mK. In contrast, the thermal conductivity of porous YSZ ceramic declined with increasing porosity, reaching a low value of 0.06 W/mK for Sample A, which had a porosity of 76%. The good agreement between the experiment data and EMT-calculated values may derive from the “interconnected” structure of porous YSZ ceramics: pores and ceramic grains were distributed randomly, with neither component necessarily continuous or dispersed. Each component may form heat conduction pathways, depending on the volume fraction of the components. Therefore, this structure could be said to have “interconnected” components. The effective conductivity of such an “interconnected” type of structure can be modeled well by the EMT equation, as established previously [14].

The observed decline in thermal conductivity with increasing temperature could be explained by the microstructures developed within the porous YSZ ceramic: the large number of pores trapped air, which is a better thermal insulator (i.e., lower thermal conductivity) than zirconia, and these air-filled pores constituted obstacles against the heat transfer along the direction of thickness; moreover, large amounts of interconnected pores made the ceramics grains not necessarily continuous or dispersed, blocking the heat conducting pathways and also contributing to the remarkably low level of thermal conductivity; in addition, the large number of pores and micro-sized interfaces provided significant phonon and photon scattering.

The thermal conductivities for a range of zirconia-based materials are expanded in the present work. The thermal conductivity of zirconia-based materials strongly depends on their microstructural features, which vary significantly with different fabrication methods. Although porous zirconia ceramic with low thermal conductivities (0.13–0.55 W/mK) was prepared by mixing YSZ suspension with latex [14], the nanoparticles were costly. Thermal conductivities of 0.55–1.40 W/mK were obtained from electron beam-physical vapor deposited (EB-PVD) ceramic

coatings (porosity, 22%) which were doped with lanthania. Plasma-sprayed TBCs and EB-PVD TBCs generated the thermal conductivities of 0.80–1.10 and 1.50–1.90 W/mK, respectively [21, 22]. The thermal conductivities of bulk YSZ were 2.20–2.90 W/mK. In contrast, porous YSZ ceramics fabricated by TBA-based gel-casting process yielded material with much lower thermal conductivities, 0.06–0.42 W/mK, which were close to the thermal conductivity of air.

Conclusions

The TBA-based gel-casting process was used to lower the thermal conductivity of porous YSZ ceramics for potential application in bulk thermal isolators. The results revealed that the porous YSZ ceramics had high porosity and uniform porous structure. These pores constituted obstacles against the through-thickness heat transfer propagation and consequently contributed to ultra-low thermal conductivity. Moreover, the experimental thermal conductivities were in good agreement with the theoretical values derived from the EMT equation. The agreement may derive from the “interconnected” structure of porous YSZ ceramics; the EMT equation is known to be a good model for such structure.

Acknowledgements This work was supported by the National Natural Science Foundation of China (Grant No: 90816019), the Natural High Technology Research and Development Program of China (“863” Program, Grant No: 2007AA03Z435), and State Key Development Program of Basic Research of China (“973” program, Grant No: 2006CB605207-2).

References

1. Ravichandran KS, An K, Dutton RE, Semiatin SL (1999) *J Am Ceram Soc* 82(3):673
2. Garrido LB, Albano MP, Plucknett KP, Genova L (2009) *J Mater Proc Tech* 209:590
3. Sakka Y, Tang F, Fudouzi H, Uchikoshi T (2005) *Sci Tech Adv Mater* 6:915
4. Gain AK, Song HY, Lee BT (2006) *Scr Mater* 54:2081
5. Jun IK, Koh YH, Kim HE (2006) *Mater Lett* 60:878
6. Hoh YH, Sun JJ, Kim HE (2007) *Mater Lett* 61:1283
7. Boaro M, Vohs JM, Gorte RJ (2003) *J Am Ceram Soc* 86(3):395
8. Rambo CR, Cao J, Sieber H (2004) *Mater Chem Phys* 87:345
9. Ryskhewitch E (1953) *J Am Ceram Soc* 36:65
10. Gu YF, Liu XQ, Meng GY, Peng DK (1999) *Ceram Int* 25:705
11. Hamling BH, Schaffer PC (1972) *Am Ceram Soc Bull* 51(4):426
12. Hamling HC, Hamling BH (1984) *Am Ceram Soc Bull* 63(8):1016
13. Claussen N, Ruhle M, Heuer A (1983) *Science and technology of zirconia II*. The American Ceramic Society, Inc., Columbus
14. Nait-Ali B, Haberkö K, Vesteghem H, Absi J, Smith DS (2006) *J Eur Ceram Soc* 26:3567
15. Chen RF, Huang Y, Wang CA, Qi J (2007) *J Am Ceram Soc* 90(11):3424
16. Hashin Z, Shtrikman S (1962) *J Appl Phys* 33:3125
17. Cao XQ, Vasseh R, Stoeber D (2004) *J Eur Ceram Soc* 24:1
18. Weast RC (1974) *Handbook of chemistry and physics*. CRC Press, Cleveland, OH
19. James KC, Simon JL, David JT, Andrew CC (2005) *Int J Heat Mass Transf* 48:2150
20. Landauer R (1952) *J Appl Phys* 23:779
21. Nicholls JR, Lawsona KJ, Johnstoneb A, Rickerbyb DS (2002) *Surf Coat Technol* 151:383
22. Matsumoto M, Yamaguchi N, Matsubara H (2004) *Scr Mater* 50:867